Int J Adv Manuf Technol (2016) 87:853–858
DOI 10.1007/s00170-016-8454-2

ORIGINAL ARTICLE

Study on the grain damage characteristics of brazed diamond grinding wheel using a laser in face grinding

Zhibo Yang[1] · **Zhen Zhang**[1] · **RuiYun Yang**[1] · **Aiju Liu**[1]

Received: 22 October 2015 / Accepted: 1 February 2016 / Published online: 1 March 2016

Abstract This paper describes the grain damage characteristics of a grinding wheel with laser-brazing and discusses its relationship to the normal grinding force during the face grinding of granite. The results of our experiment show that the primary wears patterns of the brazed diamond grinding wheel in the whole grinding process are whole, wear-away, micro-fractured, and macro-fractured. There is no type of falling-off for the diamond grinding wheel, so the result indicates that it is possible to braze the diamond grits through appropriately manipulating the parameters of the laser. During the grinding process, the diamond shapes cause grinding forces to vary, and these variations actuate the transformation of the diamond shapes. The results obtained in this paper provide a reference for researching the wear mechanism of diamond grains, for optimizing grinding parameters, and for consummating the manufacture of laser brazed diamond tools.

Keywords Diamond grinding wheel · Grinding force · Grain damage · Damage characteristics · Surface morphology

1 Introduction

There have been many developments of high-efficiency grinding techniques, especially those with high and ultra-high speeds [1–4]. At the same time, those high-temperature brazing diamond grinding wheels with high bonding strength and high grit exposing height are widely used for research. In western countries, experts have been creating of a new generation of diamond tools since the 1990s, attempting to replace plating with high-temperature brazing [3–5]. In China, researchers at Nanjing University of Aeronautics and Astronautics have also made progress in the study of high-temperature brazing diamond grains. At present, the manufacturing of high-temperature brazed monolayer diamond tools is mainly conducted through welding in a vacuum furnace or high-frequency induction welding [6–12]. However, both methods are limited in practice. For welding in a vacuum furnace, the workpiece is slow to heat and cool, lengthening in the production cycle and consuming more time and energy. In this method, the diamond grains stay in a high-temperature environment for a long period of time, risking thermal damage. Large-size tools may not be applicable due to the size of the vacuum furnace and thin-wall tools with unpredictable deformation under heat are also not a proper option. For the high-frequency induction brazing method, the advantages include fast heating, fast cooling, and shorter brazing cycles. But, the induction coil must be redesigned for tools with different shapes. The design of the gas production mechanism is more complicated for large tools or tools with special characteristics [9–17]. In the present research, a laser was chosen as the heat source. The innovative methods of manufacturing high-temperature brazing diamond tools are also discussed. The advantages of laser-brazing are selective heating areas, smaller heat-affected zones, and very slight deformation of the base after brazing, especially for plate-shaped bases, due to the flexibility of the laser head. Besides, the application of laser-brazing significantly enhances the efficiency of manufacturing the diamond grinding tools. Such enhancement will allow for the industrialization of

✉ Zhibo Yang
yangzhibo2001@163.com

[1] Henan Polytechnic University, Jiaozuo, Henan 454000, China

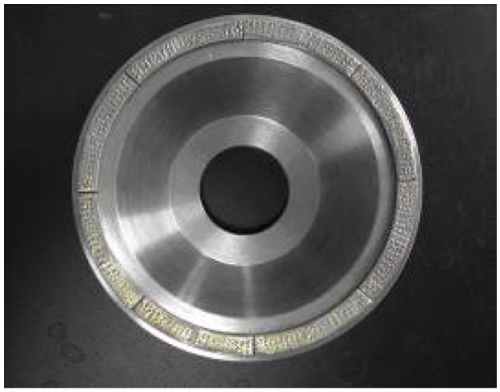

(a) The whole graphs

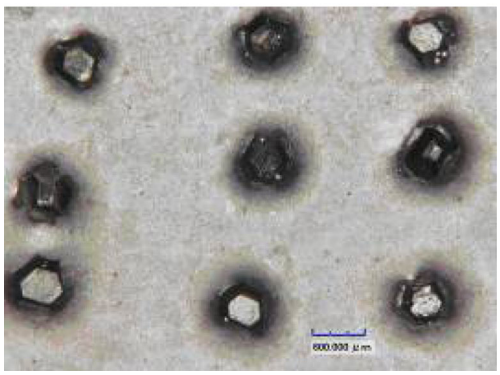

(b) Local magnification

Fig. 1 The overall morphology of the laser-brazing diamond grinding wheel

ultra-hard grinding tools and provide social and economic benefits [14–22].

For our study, Ni-creative brazing alloy was used as the connection material with a laser as the heat source. With those parameters, single-layer brazing diamond end grinding wheels were created for analysis. The grains' abrasions on the wheels, as well as the grinding forces, were observed and recorded. The wheels' grinding performances were accessed based on the gathered data. The mutual influences between the damage on grains and the grinding forces were then further studied. This research is expected to be a practical reference for choosing proper manufacturing methods of laser-brazing diamond tools in the future and their industrialization.

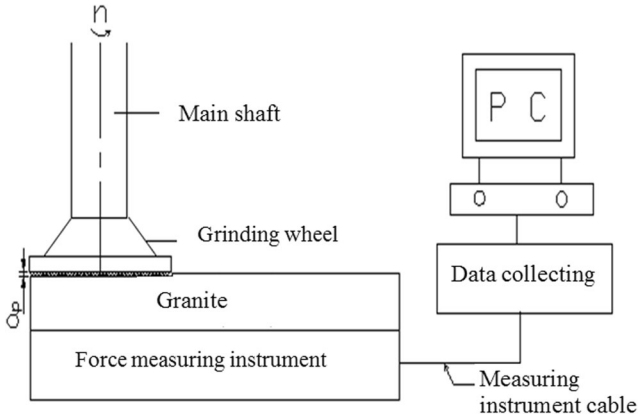

Fig. 2 Layout of the instruments

2 Instruments and methods

The experiments were conducted on a SYM-10 special-shaped stone polishing machine (main axial speed $n = 3800$ r/min, output power $P = 4.0$ kW). The parameters of the end grinding wheel used in the experiments (as shown in Fig. 1a) are an outer diameter of 104 mm, an inner diameter of 84 mm, and a working width of 6 mm.

The base of the grinding wheel was 45 steel. The brazing material was Ni-based alloy (Ni-Cr-B-Si, self-made). The size of diamond abrasive was 40/45. The brazing was conducted under the protection of argon, with optimized laser-scan parameters. After the laser-scan brazing, the diamond grains were uniformly distributed on the base of grinding wheel, as shown in Fig. 1b. The circumferential interval was approximately 2 mm. The roundness error of the grinding wheel is less than 5 um. The face grinding length was 400 mm, and the width was 100 mm.

The grinding tests were carried out in the precision grinder (M6025C), according to the criteria given in Table 1. The normal grinding force signals were collected with a Kistler 9265B dynamic force-measuring instrument. This instrument had a measuring range of −15 ~ 15 KN in all three directions. Its sampling frequency was 10 KHz at maximum. A data collection card gathered the signal data and diverted it into a charge amplifier, then into a computer for process through A/D conversion. Figure 2 shows the layout of the instruments.

Table 1 The grinding experiment parameters of the laser-brazing diamond grinding wheel

Items	Criteria
Materials	Sichuan red granite (density 2.58 g/cm^3, shore's hardness HS 92), $L = 0.5$ m
Way of cooling	Water cooling
Grinding pattern	Face grinding
Measurement of forces	The normal force was measured
Grinding feed	Feeding speed $Vw = 2$ m/min, depth of cut $a_p = 80$ μm
Morphology	The grain's morphology was examined with a 3D video microscope

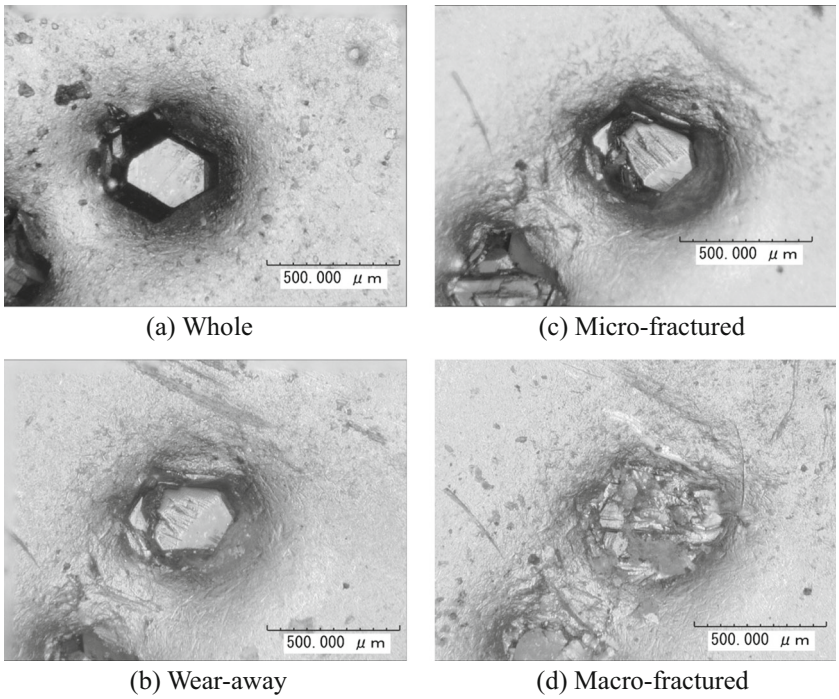

(a) Whole (c) Micro-fractured

(b) Wear-away (d) Macro-fractured

Fig. 3 The variations of damage patterns on grains

3 Results and analysis

3.1 The variation of diamond grain cutting edge in grinding

The damage characteristics of the diamond grains varied from the beginning of the grinding process until the failure of the apparatus. The damage was examined with a 3D video microscope. The examination was taken each time at the grinding sections after dual-way grinding. The damage characteristics from each time period were compared and analyzed. According to the experiment results, the damage characteristics of a grain in the process were wear-away, micro-fractured, and macro-fractured. There is no type of falling-off during the process. Those grains displaying wear-away or micro-fractures were still usable in the grinding process, since the fractures actually created new cutting edges, benefitting the entire grinding process. Figure 3 shows the variation of typical damage characteristics of one particular grain on the grinding wheel.

In the experiments, the wearing processes of 64 diamond grains were accessed. Those 64 grains were distributed in eight sections at 45-degree angles to each other. This was to ensure that they represented the general features over the grinding wheel. The results indicated that the variation of the wearing features was from whole, to wear-away, to micro-fractured (local fragmentation occurred), ending at macro-fractured (the fragmentation of the whole grain occurred), as shown in Fig. 3. Further observation of the grains' features revealed that there were two other patterns aside from those mentioned above. The two new patterns

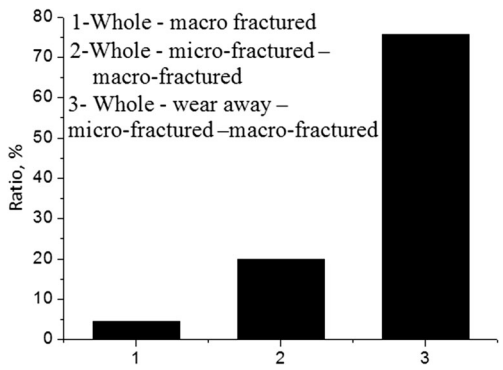

Fig. 4 The distribution of each damage patterns

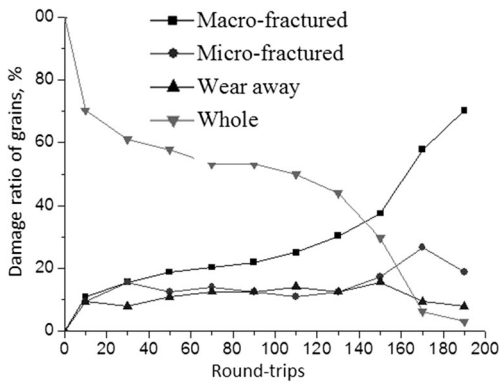

Fig. 5 The variation of each damage patterns during the process of grinding

were (1) whole-macro-fractured and (2) whole-micro-fractured-macro-fractured.

Figure 4 gives the distribution of all the three damage patterns. Due to very low ratio in the existence composition, the whole-macro-fractured pattern was determined as an abnormal failure of the diamond grains. The whole-micro-fractured-macro-fractured pattern held a higher ratio than the former one, but was still generally low. In this pattern, the alternative thermal stress, the alternative impacts, and the uneven strength of the grain itself all played vital roles in pushing the grain toward a shorter lifetime.

The grains' morphological data at different spots during the grinding process were obtained and analyzed for their variation trends. In the experiment, the wheel failed after approximately 190 rotations. Figure 5 gives the composition ratio of each damage pattern under different numbers of rotations.

From Fig. 5, we see that the ratios of macro-fractured, micro-fractured, and wear-away damages all increased significantly in the early stage. This is because some grains were above the average height, meaning they were the first ones affected by the grinding. In such an early stage, only a few grains were involved in the process, so the load on each grain was massive. Under the grinding forces, those grains were rapidly damaged or fractured. So, the curves in the early stage are quite steep. In the middle stage, the ratios of micro-fractured and wear-away damages trended to be flat and stable. The ratio of macro-fractured damages increased gradually. Wear-away damages became micro- or macro-fractured, while micro-fractured damages transitioned into wear-away or macro-fractured. This explains why both the wear-away curve and the micro-fractured curve flatten during the middle stage. In the late stage, after 150 round trips, more grains were damaged and grew in size as the grinding force caused further deterioration. This is why the ratio of macro-fractured damages increased sharply in this stage. Putting the results from the three stages together, we can say that the diamond grains passed through the stages of initial wear, normal wear, and severe wear.

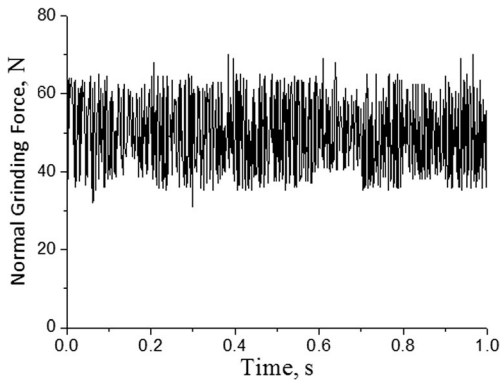

Fig. 6 The Grinding force's wave pattern, from a grinding wheel at the stable stage

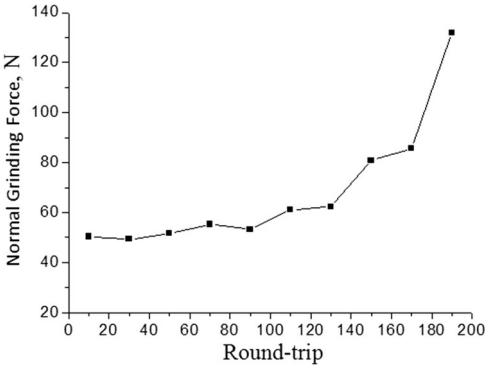

Fig. 7 The average normal grinding force on the wheel

3.2 Analysis to the relationship between wheel's surface morphology and grinding force

During the grinding process, the entire surface of the wheel was in contact with the stone. The tangential resistance force was offset in the opposite direction. Thus, we concluded that only a normal grinding force was necessary for analysis. The size of the normal force depended on the sharpness of the grinding wheel. Figure 6 gives the grinding force's wave pattern from the surface of a laser-brazing diamond grinding

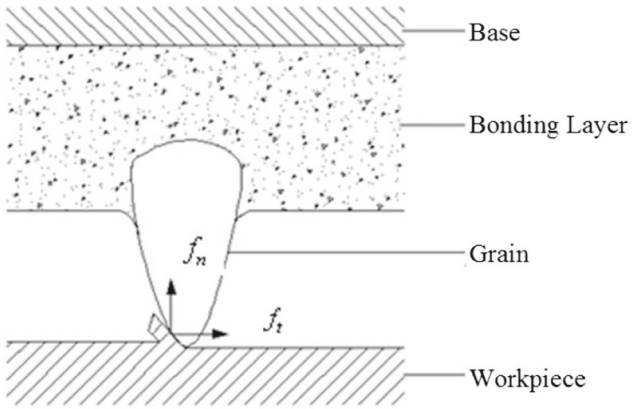

(a) A Sharp Grain

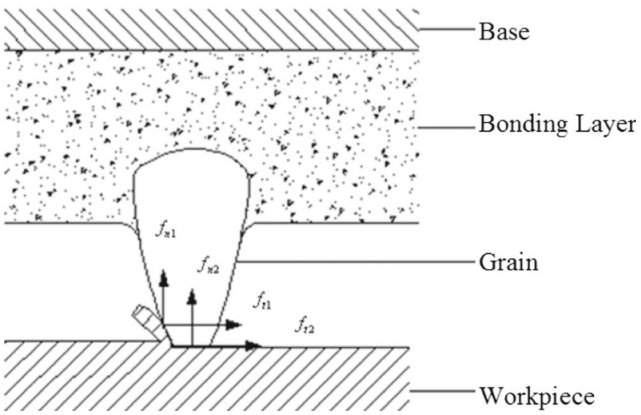

(b) A Wear Grain

Fig. 8 The grinding forces applied on two different grains

wheel during the tenth rotation. In correspondence with Figs. 5 and 7, it shows the variation of the average normal grinding force F_n on the wheel surface during the stable stage.

We can tell from Fig. 7 that the grinding force increased as the process continues; this is because the grain begins with a sharp cutting edge. There were forces, a horizontal component f_t and a vertical component f_n, applied on the edge, as shown in Fig. 8a. This caused the edge to cut into the workpiece, removing materials. As the grinding process went on, the tip of the edge was worn off, which brought in another friction force onto the wear-top. As shown in Fig. 8b, in addition to the already presented components, f_{t1} and f_{n1}, there were also a frictional horizontal component f_{t2} and a vertical component f_{n2} applied to the wear-top as a result of its contact with the workpiece. We assumed that the area of the wear-top was A_g and the part of workpiece in contact as it was already in yield state. If the compressive yield stress of the workpiece was δs, then there was a vertical component $f_{n2} = A_{g\delta s}$. A conclusion was drawn that the variation of the grinding force was caused by the variation of the top area.

Figure 7 shows that the normal grinding force increased gradually in the early stage and maintained a relatively stable state thereafter. It resumed its rapid increase in the late stage, since many macro-fractured grains appeared in this stage. The total amount of grains was reduced. So, the non-deformed cutting thickness for each grain increased, as did the grinding force itself. During the entire process, the grinding force changed continuously with the variation of the wheel's damage characteristics.

From the analysis on both damage characteristics and grinding forces, we see that there is a sound relationship between the change of ratios of different damage states and the variation of grinding forces. In other words, the grinding force is small when more of the grains are whole or show wear-away damages, only a few of them are whole or wear-away damaged ones.

4 Conclusion

(1) During the process of grinding granites with laser-brazing diamond grind wheels, the grains passed through states of damages including macro-fractured, micro-fractured, and wear-away. Grains that fell off the wheel were not found in observation.

(2) During the process, as the number of rotations increased, the grinding force increased and maintained a stable state for a certain period of time. The force rapidly increased once again in the late stage. Our study showed that the grinding force was more closely related to whole, macro-fractured, and micro-fractured damages; the grinding force is small when more of the grains are whole or show wear-away damages.

(3) Laser-brazing did provide a high bond between the diamond and the base. The general pattern of variation was whole-wear-away-micro-fractured-macro-fractured.

Acknowledgments This research was supported by the financial supports from the National Natural Science Funds Fund (U1204517), Natural Science Fund by the Education Department of Henan Province P.R. China (12B460011), and the Opening Project of Key Laboratory of Precision Manufacturing Technology and Engineering, Henan Polytechnic University.

References

1. Kopac J, Krajnik P (2006) High-performance grinding—a review. J Mater Process Technol 175:278–284
2. Azarhoushang B (2014) Wear of non-segmented and segmented diamond wheels in high-speed deep grinding of carbon fibre-reinforced ceramics. Int J Adv Manuf Technol 74:1293–1302
3. Jackson MJ, Davis CJ, Hitchiner MP, Mills B (2001) High-speed grinding with CBN grinding wheels—applications and future technology. J Mater Process Technol 110:78–88
4. Yang ZB, Xu JH, Liu AJ (2009) Microstructure and formation mechanism of diamond abrasive grain interface by laser brazing of Ni-based alloy. Chin J Lasers 36(11):3079–3083
5. Chen JY, Xu XP (2014) Tribological characteristics in high-speed grinding of alumina with brazed diamond wheels. Int Adv Manuf Technol 71:1579–1585
6. Chen JY, Shen JY, Huang H, Xu XP (2010) Grinding characteristics in high speed grinding of engineering ceramics with brazed diamond wheels. J Mater Process Technol 210:899–906
7. Chattopadhyay AK, Chollet L, Hintermann HE (1991) On performance of brazed bonded monolayer diamond grinding wheel. Ann CIRP 40(1):347–350
8. Dai JB, Ding WF, Zhang LC, Xu JH, Su HH (2015) Understanding the effects of grinding speed and undeformed chip thickness on the chip formation in high-speed grinding. Int J Adv Manuf Technol 81:995–1005
9. Meng WR, Xu KW, Nan JM (2004) Monolayer diamond tools brazed with active filler. Rare Metal Mater Eng 33:771–774
10. Buhl S, Leinenbach C, Spolenak R, Wegener K (2010) Influence of the brazing parameters on microstructure, residual stresses and shear strength of diamond-metal joints. J Mater 45(16):4358–4368
11. Qiu WQ, Liu ZW, He LX, Zeng DC, Mai YW (2012) Improved interfacial adhesion between diamond film and copper substrate using a Cu(Cr)-diamond composite interlayer. Mater Lett 81(15): 155–157
12. Ma BJ, Lou JP, Pang Q (2014) Brazed diamond micropowder bur fabricated by supersonic frequency induction heating for precision machining. J Mater Eng Peformance 23:1505–1510
13. Amei KJ, Tomohiro Y, Takahisa OJ (2015) Restraint method for overcoming heating irregularity and improving heating equipment efficiency for beverage cans using high-frequency induction heating. Electr Eng Jpn 192(2):22–30
14. Peng HE, Feng JC, Liu HJ (2003) Optimization design of electromagnetism induction heating technical parameters in high frequency induction brazing. Trans Nonferrous Metals Soc China 13(1):34–38
15. Yao ZJ, Su HH, Fu YC (2005) High temperature brazing of diamond tools. Trans Nonferrous Metals Soc China 15(6):1297–1302
16. Bemardus SA, Christian L, Christoph K (2015) Processing of metal-diamond-composites using selective laser melting. Rapid Prototyp J 21:130–136

17. Yang ZB, Liu AJ, Xu JH (2010) Laser brazing diamond grinding wheel with Ni-base filler alloy. Adv Mater Res 139:218–221
18. Ma BJ, Xu HJ, Fu YC (2004) Study on the grain damage characteristics of diamond quills in face grinding. China Mech Eng 6: 1085–1087
19. Zhan YJ (2006) Experimental study on surface grinding with brazed diamond tools. Thesis of Master's Degree 4:37–42
20. Hwang TW, Evans CJ, Malkin S (2000) High speed grinding of silicon nitride with electroplated diamond wheels. ASME J Manuf 122:42–50
21. Zhang YZ (1988) Theories of metal cutting. Aviation Industry Press, Beijing. pp 385–386
22. Wale VY, Patil RN (2013) Modeling and simulation of surface grinding process for comparing the performance of coolants used. Int J Next Gener Comput Appl 1(9):13–18